Genomic Insights into Fertilization: Tracing PLCZ1 Orthologs Across Amphibian Lineages

Rachel E. Bainbridge [1,†], Joel C. Rosenbaum [1,†], Paushaly Sau [1], Anne E. Carlson [1,*]

[1]Department of Biological Sciences, University of Pittsburgh, Pittsburgh, PA 15260, USA

*Corresponding author: E-mail: acarlson@pitt.edu.

[†]These authors contributed equally to this work.

Accepted: February 26, 2025

Abstract

Fertilization triggers a cascade of events, including a rise in egg cytosolic calcium that marks the onset of embryonic development. In mammals and birds, this critical process is mediated by the sperm-derived phospholipase C zeta (PLCζ), which is pivotal in releasing calcium from the endoplasmic reticulum in the egg and initiating embryonic activation. Intriguingly, *Xenopus laevis*, a key model organism in reproductive biology, lacks an annotated *PLCZ1* gene, prompting questions about its calcium release mechanism during fertilization. Using bioinformatics and RNA sequencing of adult *X. laevis* testes, we investigated the presence of a *PLCZ1* ortholog in amphibians. While we identified *PLCZ1* homologs in 25 amphibian species, including 14 previously uncharacterized orthologs, we found none in *X. laevis* or its close relative, *Xenopus tropicalis*. Additionally, we found no compensatory expression of other PLC isoforms in these species. Synteny analysis revealed a *PLCZ1* deletion in species within the Pipidae family and another intriguing deletion of potential sperm factor *PLCD4* in the mountain slow frog, *Nanorana parkeri*. Our findings indicate that the calcium release mechanism in frog eggs involves a signaling pathway distinct from the PLCζ-mediated process observed in mammals.

Key words: comparative genomics, phylogenetics, reproductive biology, *Xenopus*, phospholipase C.

Significance

This study reveals the absence of the sperm enzyme PLCζ in the African clawed frog (*Xenopus laevis*), providing new insights into the diversity of genetic mechanisms underlying egg activation and fertilization. This finding highlights the evolutionary adaptability of reproductive processes across species. Our findings invite a reevaluation of genetic models of reproduction, highlighting how genomic variations shape crucial processes at the beginning of new life.

Introduction

For most animals, fertilization triggers a surge in the calcium levels within the egg cytoplasm that begins near the site of sperm entry and permeates the entire egg (Steinhardt et al. 1977; Gilkey et al. 1978). This calcium catalyzes essential processes that prevent polyspermy and initiate embryonic development (Denninger et al. 2014; Swann and Lai 2016). Among the hypothesized mechanisms for this signal in mammals (Saunders et al. 2002; Nomikos et al. 2017) and birds (Coward et al. 2005) is the release of the sperm-derived enzyme phospholipase C zeta (PLCζ) into the egg. PLCζ cleaves the phospholipid phosphatidylinositol 4,5-bisphosphate (PIP_2) to release soluble inositol trisphosphate (IP_3) within the egg, which then

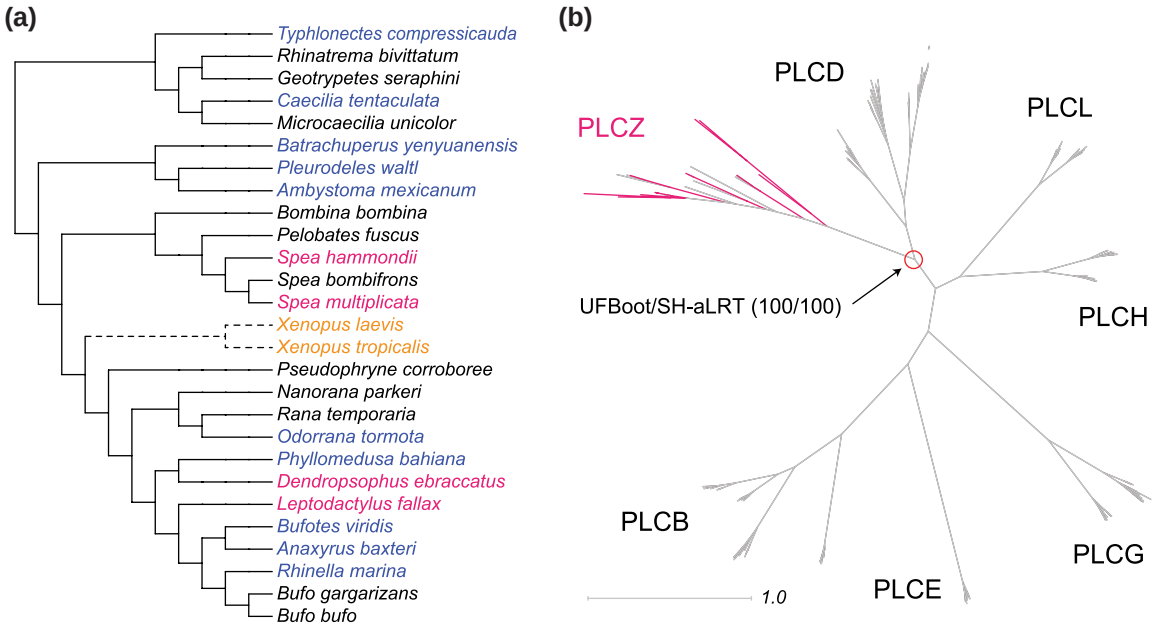

Fig. 1. Identification of amphibian PLCζ isozymes and characterization of PLC orthologs in amphibians. a) Cladogram illustrating the occurrence of *PLCZ1* orthologs in amphibian species. Annotated orthologs are colored black, orthologs identified in transcriptome assemblies are blue, those identified in WGS assemblies are pink, and species missing orthologs are orange. b) Unrooted phylogram illustrating the alignment of newly identified PLCZ1 orthologs (pink) with annotated amphibian PLCs. Bootstrap support values for branching at the PLCZ node are highlighted.

initiates the release of calcium from the endoplasmic reticulum (ER) (Cox et al. 2002; Saunders et al. 2002; Yoneda et al. 2006; Mizushima et al. 2007; Ito et al. 2008; Ross et al. 2008; Bedford-Guaus et al. 2011; Mizushima et al. 2014). While ER-derived calcium is pivotal for egg activation in most animals (Crossley et al. 1988; Whitaker 2006), it remains uncertain whether the PLCζ-anchored mechanism is similarly widespread.

The African clawed frog (*Xenopus laevis*) is a long-standing and fundamental model organism for fertilization research. Similar to mammals and birds, fertilization in *X. laevis* eggs induces an increase in cytosolic calcium (Grey et al. 1982; Kline 1988). This calcium surge triggers the fast and slow blocks to polyspermy (Wozniak, Phelps, et al. 2018; Wozniak and Carlson 2020) and sets embryonic development in motion (Whitaker 2006). Despite these similarities, no PLCζ-encoding gene (*PLCZ1*) has been identified in the genomes of *X. laevis* or the related *Xenopus tropicalis*. While PLC activation is integral for this process (Wozniak, Tembo, et al. 2018), our previous studies found no evidence of activation in the PLC isoforms (Plcg1, Plcb1, and Plcb3) expressed in *X. laevis* eggs during fertilization (Komondor et al. 2023). One possibility is that *X. laevis* sperm donates an unidentified soluble sperm factor like PLCζ to the egg, as occurs in mammals and birds. Notably, *X. laevis* sperm extracts introduced into mouse eggs produce a calcium rise comparable to that caused by chicken or cow sperm extracts (Dong et al. 2000). Using a comparative genomics and transcriptomics approach, we set out to identify potential sperm factors in *Xenopus* and other amphibian species with readily available genome or transcriptome assemblies.

Results

At the outset of our study, we searched for genes encoding PLCζ in amphibians. Our initial analysis revealed only 11 annotated amphibian *PLCZ1* orthologs, making it the least represented among all tetrapod classes (Fig. 1a). To broaden our investigation, we employed tblastn using the protein sequence of *PLCZ1* from the plains spadefoot toad (*Spea bombifrons*) as a query against the NCBI transcriptome shotgun assembly (TSA) database and other transcriptome databases (Table 1). Additionally, we searched for *PLCZ1* in amphibian whole genome shotgun (WGS) assemblies, using miniprot (Li 2023) to identify open reading frames. We required a query coverage of greater than 30% to consider identified sequences for further analysis (Table 2). These comprehensive searches identified not only *PLCZ1* but also *PLCD1-4* orthologs.

We differentiated these orthologs through multiple sequence alignment (MSA) and phylogenetic analysis alongside all annotated amphibian PLC isozymes. When grouped by clade, these sequences appeared across all 3 amphibian orders: tailless frogs and toads (*Anura*), newts and salamanders (*Urodela*), and limbless caecilians (*Gymnophiona*). However, we were unable to recover

Table 1 PLCZ1 orthologs from TSA assemblies

Species	PLCD1	PLCD3	PLCD4	PLCZ1	TSA%
Odoranna tormota	GGLB01015957.1	GGLB01130168.1	GICS01011310.1	GGLB01190867.1	ND
Phyllomedusa bahiana	GJVR01002153.1	GJVR01021158.1	JAODAL010011353.1	GJVR01006992.1	86.3%
Bufotes viridis	GDRL01009328.1	GDRL01076335.1	GDRL01023503.1	GDRL01074809.1	87.0%
Anaxyrus baxteri	GGUR01113776.1	GGUS01070471.1	…	GGUS01004549.1	75.0%
Rhinella marina	GFMT01054478.1	GFMT01011327.1	GFMT01015328.1	GFMT01012350.1	90.0%
Ambystoma mexicanum	GFBM010738982.1	GFZP01060979.1	GFBM010701881.1	GFBM010729806.1	88.0%
Batrachuperus yenyuanensis	…	…	…	GHDZ01000855.1	40.0%
Thyphlonectes compressicauda	GFOH01022246.1	GFOH01039492.1	…	GFOH01055956.1	98.0%
Caecilia tentaculate	GFOD01029325.1	GFOD01040826.1	GFOD01011139.1	GFOD01009484.1	97.0%
Pleurodeles waltl	M0253040_PLEWA04	M0088963_PLEWA04	M0481258_PLEWA04	M0188898_PLEWA04	99.0%

Table 2 PLCZ1 orthologs from WGS assemblies

Species	Accession	Start	End	Query species	Cover	Query%	N50
Dendropsophus ebraccatus	JAQFWZ010000097.1	956,047	1,049,656	*S. bombifrons*	76 to 694	89.1	10,560,916
Leptodactylus fallax	CAMRHE010000770.1	57,323	104,851	*S. bombifrons*	114 to 694	83.6	4,630,249
Spea hammondii	JARDYJ010000004.1	201,062	211,324	*S. bombifrons*	1 to 694	100	14,335,781
Spea multiplicata	VKOC01030321.1	6,776	1,982	*S. bombifrons*	8 to 425	60.1	30,692
Calotriton arnoldii	CAWUFW010000241.1	3,392,081	3,489,269	*B. yenyuanensis*	58 to 239	28.5	1,599,425
Desmognathus carolensis	JASAFM010328747.1	95	337	*B. yenyuanensis*	108 to 190	13.1	806
Desmognathus fuscus	JASBQP010655945.1	277	468	*B. yenyuanensis*	554 to 620	10.4	849
Desmognathus catahoula	JAVHNH011175711.1	317	559	*B. yenyuanensis*	108 to 190	13.1	858
Desmognathus tilleyi	JAWLIA012642144.1	162	353	*B. yenyuanensis*	554 to 620	10.4	677

PLCZ1 orthologs from many TSA datasets, likely because *PLCZ1* expression is typically restricted to the testes (Cox et al. 2002; Nomikos et al. 2005). Despite the presence of testis tissue in several *Xenopus* transcriptome assemblies, no evidence of *PLCZ1* was detected (Fig. 1a).

Our initial search for *PLCZ1* uncovered many *PLCD1-4* transcripts, which became apparent when we aligned the sequences to annotated amphibian PLCs. We similarly found *PLCD1-4* genes in our search within WGS assemblies. Phylogenetic analysis distinguished *PLCZ1* orthologs from *PLCD1-4* with robust bootstrap support (Fig. 1b; supplementary fig. S1, Supplementary Material online), reinforcing our original classifications. However, there remained a concern regarding the potential misidentification of *PLCD1-4* as *PLCZ1* due to their pronounced similarities. Additionally, some *PLCD1-4* transcripts might lack the sequence encoding the determinative pleckstrin homology domain due to RNA-sequencing errors (Wang et al. 2009).

To further validate our findings, we performed a separate search for *PLCD1-4* in the transcriptome assemblies where we had previously detected *PLCZ1*. *PLCD1* and *PLCD3* were found in all queried species except the Yenyuan stream salamander (*Batrachuperus yenyuanensis*), possibly explained by the low completeness (40.1%) of its assembly (Xiong et al. 2019). More surprisingly, we discovered species lacking a gene encoding PLCD4. This enzyme is expressed in multiple *X. laevis* tissues, including the testis (Bowes et al. 2010; Session et al. 2016), and is integral to the acrosome reaction in mammalian sperm (Fukami et al. 2001; Table 1).

To understand how anurans lacking *PLCZ1* and *PLCD4* diverged from related species, we examined their conserved synteny, which refers to the conservation of gene blocks on chromosomes across different species. We identified a shared synteny block containing *PLCZ1* in the common frog (*Rana temporaria*), common toad (*Bufo bufo*), and the plains spadefoot toad (*S. bombifrons*). Using gene anchors from this block, we compared these species and frogs from the Pipidae family, including 3 *Xenopus* species and the Congo dwarf clawed frog (*Hymenochirus boettgeri*) (Fig. 2a). For assemblies lacking annotations, we used miniprot (Li 2023) to identify genes (Table 3). Our data showed that every available assembly from Pipidae lacks *PLCZ1*, indicating a gene deletion in that family's ancestral lineage.

We also reanalyzed species from our ortholog search to locate a syntenic block for *PLCD4*. In the mountain slow frog (*Nanorana parkeri*), this block revealed a gene deletion, although it does not occur in other members of its family (Hime et al. 2021; Fig. 2b).

We performed a transcriptomics analysis on *X. laevis* to assess the expression of various potential sperm factors and to detect potential unannotated *PLCZ1* orthologs. Our best understanding of PLCζ function comes from studies in mammals, where it is exclusively found in sperm (Session et al. 2016). Mature sperm are transcriptionally quiescent (Kierszenbaum and Tres 1975), rendering them unsuitable for transcriptomics. Therefore, we opted to perform RNA-seq on whole testes. While we acknowledge that

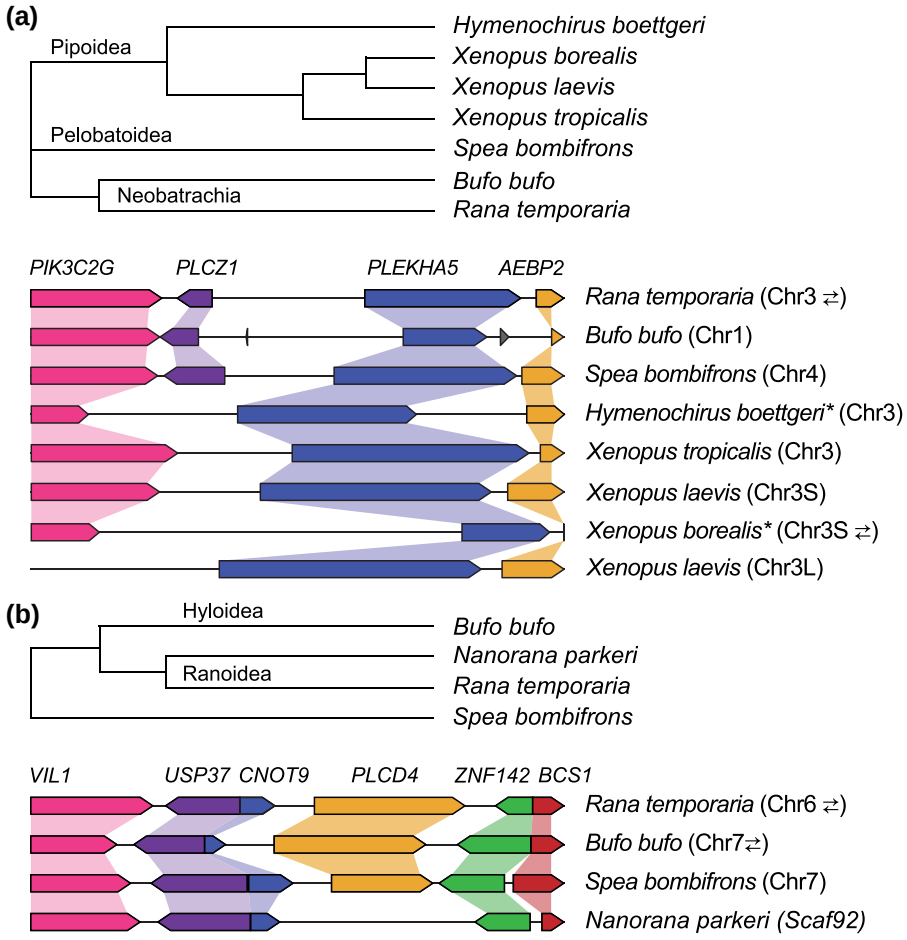

Fig. 2. Synteny analysis of PLCZ1 and PLD4 loci. a) Local synteny comparison around the *PLCZ1* locus suggests its deletion in species from the Pipidae family. The chromosome source for each block is noted in parentheses. Blocks marked with an ⇄ symbol have had their order reversed for clarity. Species with an asterisk (*) signify incomplete assemblies for that region, with coverage and annotation methods detailed in Table 3. b) The local synteny comparison for the *PLCD4* locus indicates a deletion in *N. parkeri*.

not all RNA in the testes translates to proteins in sperm, RNA encoding sperm proteins should be present within the testis. For our analysis, we extracted RNA from the testes of 3 adult *X. laevis* males. Following library preparation and sequencing, we produced an average of 66,723,678 contiguous RNA-seq reads per biological replicate, with 48% to 51% aligned to the *X. laevis* genome. We observed at least 1 transcript in 1 testis from an individual frog for 33,377 genes. We performed gene ontology (GO) analysis on 6,000 of the most highly expressed genes among these testis-derived transcripts. Of these, 48.3% were identified with GO biological process terms, many of which were essential for general cell maintenance (e.g. translation, protein folding, and cell cycle) (Table 4). Some were also involved in specialized processes such as spermatogenesis. Our overall results were highly correlated (supplementary fig. S2, Supplementary Material online) and matched a separate dataset (Fig. 3a). In our dataset, we identified several essential sperm transcripts, including deleted in azoospermia-like (*dazl*) (Houston and King 2000) and the testes-specific histone (*h1-10*) (Shechter et al. 2009; Oikawa et al. 2020). Other enriched transcripts, such as *astl2b*, *rflcii*, and *ribc1*, are known to be specifically expressed in *X. laevis* testis (Session et al. 2016) or as proteins in sperm (Sakaue et al. 2010; Ferlin et al. 2012; Agarwal et al. 2016; Maccarinelli et al. 2017). Some of these, including *rflcii*, *cfh*, and *tubb4b*, are essential for fertility in other species (Table 4; Sakaue et al. 2010; Ferlin et al. 2012; Agarwal et al. 2016; Maccarinelli et al. 2017).

We searched the RNA-seq dataset for transcripts encoding sperm factors, beginning with PLC isoforms. We identified transcripts for PLCβ, PLCδ, and PLCγ (Fig. 3b). Of these, the *plcd4* transcript was the most abundant in our dataset. Notably, *plcd4* was also the most abundant PLC transcript in testis datasets from the inbred *X. laevis* J strain (Session et al. 2016) and the *X. tropicalis* Nigerian strain, neither

Table 3 Identification of genes within unannotated synteny blocks

Assembly	Method	Query	Coverage	Match	RBH
***Hymenchrius boettgeri* (chromosome)**	miniprot	Aebp2	1 to 377 (100%)	Chr3: 4,149,416 to 4,187,276	Aebp2
	miniprot	Plekha5	1 to 1,235 (100%)	Chr3: 3,859,537 to 4,039,496	Plekha5
	miniprot	Pik3c2g	54 to 1,782 (97%)	Chr3: 3,653,235 to 3,709,345	None
	tblastn	Pik3c2g	54 to 1,782 (97%)	Chr3: 3,653,236 to 3,709,345	Pik3c2g
	tblastn	PLCZ1	74 to 691 (89%)	Chr6: 77,950,903 to 77,964,377	Plcl2
***Xenopus borealis* (chromosome)**	miniprot	Aepb2	194 to 236 (11%)	Chr3S: 11,092 to 111,048	Aebp2
	miniprot	Plekha5	72 to 1,235 (94%)	Chr3S: 117,090 to 154,425	Plekha5
	miniprot	Pik3c2g	1 to 1,641 (92%)	Chr3S: 306,811 to 334,344	Pik3c2g
	tblastn	PLCZ1	78 to 691 (88%)	Chr6S: 35,994,393 to 35,996,171	Plcl2

Table 4 Comparative gene expression in *X. laevis* testes

Gene	This study	Taira (2016)
astl2b.L	11.81	12.62
dazl.L	10.21	10.62
rflcii.S	12.55	11.09
cfh.L	9.18	9.92
h1-10.S	6.76	9.77
tubb4b.L	10.20	9.27
ribc1.S	8.29	9.86
sycp3.L	8.01	9.04
syngr4.L	89.46	9.26
pbk.L	9.53	10.12
hormad1.S	7.84	8.59
odf3.S	8.22	7.90

of which possessed a *PLCZ1* ortholog. By comparison, testes of the Oriental fire-bellied toad *Bombina orientalis* contained *PLCZ1* transcripts but also substantially reduced levels of *plcd4* compared with *Xenopus*.

In mice, we observed that *Plcz1* was the predominant PLC isoform expressed in a dataset from 3-month-old mouse testes. However, *Plcd4* levels were comparable to those found in *Xenopus* species (Fig. 3b; Huang et al. 2021). We also assessed the presence of *wbp2nl* (PAWP), a sperm head protein proposed to be involved in egg activation in both frogs (Aarabi et al. 2010) and mice (Wu et al. 2007). While mouse and *Xenopus* exhibited comparable *wbp2nl* transcript levels, *B. orientalis* lacked this transcript entirely (Fig. 3b).

To further examine the absence of *PLCZ1* in *Xenopus* species, we evaluated the unmapped RNA from our dataset for potential *PLCZ1* orthologs. We conducted a **blastx** search using the unmatched reads against a database of *PLCZ1* sequences from mammals and amphibians. This search yielded 360 reads with an *E*-value $<10^{-6}$. These reads were then aligned to a *PLCZ1* protein sequence from the neotropical leaf frog, *Phyllomedusa bahiana*, which was not included in our initial blastx database. The alignment covered residues 170 to 654 of this ortholog. However, further evaluation showed the reads were a closer match to *PLCD1-4* (Supplementary Material online). This suggests the unmapped reads in our dataset likely originate from incomplete contigs of annotated genes.

Discussion

As in other species, fertilization in *X. laevis* results in a surge of cytosolic calcium in the egg, a process facilitated by PLC enzymes that produce IP_3 to induce calcium release from the ER (Runft et al. 1999; Runft et al. 2002). Various mechanisms have been proposed for initiating this cascade of events. In mammals and birds, it is believed that sperm deliver soluble PLCζ to the egg during fertilization, serving as the trigger that initiates the calcium surge in the egg cytoplasm (Swann and Lai 2016).

Because of its role in mammalian and avian fertilization, we were surprised to find no annotated ortholog of *PLCZ1* in *X. laevis*. This prompted us to investigate, which other amphibians possess this enzyme. Using annotated genes and TSA, we successfully identified *PLCZ1* orthologs in 25 distinct amphibian species (Fig. 1b). These samples provide broad taxon coverage for amphibians, especially considering that *PLCZ1* transcripts are hypothetically constrained to the testes, a tissue type frequently absent from transcriptomics datasets.

Our inability to detect a *PLCZ1* ortholog in either *Xenopus* species implies a possible gene deletion in the *Xenopus* ancestral lineage, as corroborated by our local synteny analysis (Fig. 2a). When we included *H. boettgeri* in the analysis, a *PLCZ1* deletion in a Pipidae common ancestor became apparent. We attempted to establish this deletion's origin for all sequenced family members of Pipidae. However, we were unable to extend this analysis to Surinam toads (*Pipa*) due to incompleteness of the genomic assemblies available for these species.

We also noted the absence of *PLCD4* in *N. parkeri* (Fig. 1d). Local synteny comparison confirmed a PLCD4 deletion in this species, which appears to be a recent event since another Ranidae species, *R. temporaria*, maintains a functional version of this gene (Ma et al. 2018). We observed 3 additional species missing *PLCD4*. The Yenyuan stream salamander, with 40.1% of its transcriptome complete, and the Wyoming toad (*Anaxyrus baxteri*), at 75%

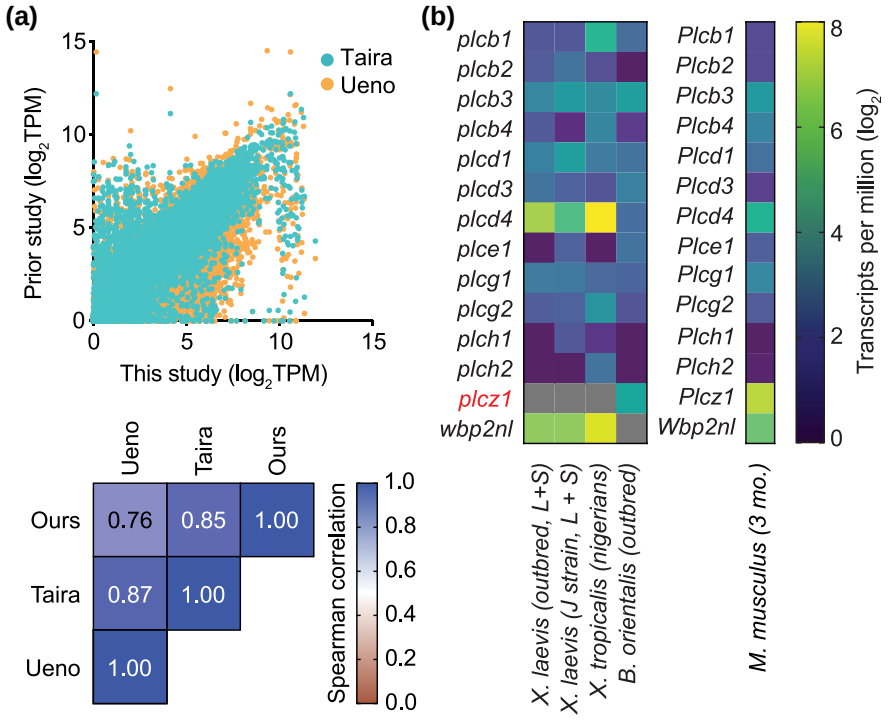

Fig. 3. Expression heatmap of sperm factors in anuran and mouse testis. a) Comparison of transcript counts between this study and previous ones (Session et al. 2016); Spearman rank correlation shown for each comparison is shown at the bottom. b) Heatmaps depicting the expression levels of annotated PLC genes from the specified animals, displayed as $\log_2$ transformed transcripts per million. Gray boxes indicate transcripts lacking annotation. For anurans, *plcz1* is highlighted in red to emphasize its absence from *Xenopus*. The putative sperm factor *wbp2nl* is also included for reference. The *X. laevis* (outbred) data is from this study, *X. laevis* (J strain) from GSE73419 (Session et al. 2016), *X. tropicalis* from GSM5230669 (unpublished), *B. orientalis* from GSE163874 (unpublished), and 3-month-old mice from GSE181426 (Huang et al. 2021).

completeness (Carlson et al. 2022), may lack *PLCD4* due to incomplete datasets. In contrast, the absence of a *PLCD4* transcript in the Cayenne caecilian (*Typhlonectes compressicauda*), with its 97.6% complete transcriptome, strongly suggests a *PLCD4* deletion, but this cannot be definitively verified without a complete genome assembly.

The absence of the PLCζ isozyme in the *Xenopus* species analyzed in this study poses significant questions regarding PLC-activated calcium release during their fertilization. While a substantial body of evidence has identified *PLCZ1* as the primary sperm factor for egg activation (Swann 2022), its absence in *Xenopus* challenges the universality of this mechanism. Beyond PLCζ, other sperm factors, such as extramitochondrial citrate synthase (CSL or eCS) (Harada et al. 2007, 2011; Kang et al. 2020) and the post-acrosomal WWP-domain-binding protein (WBP2NL or PAWP) (Wu et al. 2007), have also been proposed to initiate this process. However, we did not detect a CSL ortholog in *Xenopus* or any other anuran species. The orthologs we did find contained the targeting sequence characteristic of mitochondrial citrate synthase (CS). By contrast, PAWP is expressed in *Xenopus* testes (Fig. 3b), but its postulated role in egg activation has been contested in various studies (Nomikos, Sanders et al. 2014; Nomikos, Theodoridou et al. 2014; Nomikos et al. 2015). This leads us to consider alternative candidates like *plcd4*, which is highly expressed in testes (Fig. 3b). However, sperm from *PLCD4* knockout mice induce calcium waves in eggs after intracytoplasmic injection (Fukami et al. 2001).

We finally consider that a soluble sperm protein may not be the sole factor that increases cytoplasmic calcium in the egg. This aligns with the "receptor model" of egg activation, in which a signaling cascade is activated by binding a sperm surface ligand to an egg receptor (Jaffe 1990). *Xenopus laevis* eggs express a PLCγ isoform (Plcg1), which can be activated by phosphorylation from receptor tyrosine kinases (Sato et al. 2000; Kadamur and Ross 2013), as well as PLCβ isoforms (Plcb1 and Plcb3), which GPCRs activate (Smrcka et al. 1991; Rhee 2001). However, fertilization in *X. laevis* does not cause observable phosphorylation at the critical tyrosine residue (Y776) of Plcg1, and inhibitors of either PLCγ or PLCβ pathway did not affect the PLC mediated fast block to polyspermy (Komondor et al. 2023). Another alternative explanation is the "calcium bomb" hypothesis, which proposes that a burst of calcium is introduced to the egg with sperm entry, resulting in egg

activation and calcium release from the ER (Jaffe 1983). In other model systems, introducing calcium was insufficient to produce calcium release, indicating that other factors are required (Swann and Ozil 1994). Given these findings, it's conceivable that a combination of these mechanisms may be needed to trigger egg activation in *Xenopus* and other species successfully. Additional studies will be instrumental in identifying the factors required for egg activation, providing new insights into life's earliest events.

Materials and Methods

Ethics Statement

All animal procedures were conducted using acceptable standards of humane animal care and approved by the Institutional Animal Care and Use Committee (IACUC) at the University of Pittsburgh.

Retrieval of Amphibian *PLCZ1* Sequences

We searched for amphibian *PLCZ1* orthologs in the TSA database using tblastn queries with *PLCZ1* protein sequences from the common toad (*B. bufo*), Plains spadefoot toad (*S. bombifrons*), and Gaboon caecilian (*Geotrypetes seraphini*). Additionally, we retrieved the *Pleurodeles waltl PLCZ1* ortholog from the TSA hosted by iNewt (Matsunami et al. 2019). To expand our search, we queried amphibian WGS assemblies with tblastn to identify potential *PLCZ1* orthologs. For promising hits, we used miniprot (Li 2023) to recover full coding sequences. After pooling sequences encoding potential *PLCZ1* orthologs, we validated the candidates through a reciprocal best-hit blastx search against the nonredundant protein database, considering hits with at least 30% query sequence coverage as tentative *PLCZ1* orthologs for further analysis.

Phylogeny of Recovered PLCZ1 Orthologs

To validate our initial PLCZ1 classifications, we compared the recovered protein sequences with those of annotated amphibian PLC isozymes, generating a MSA using MAFFT (Katoh and Standley 2013). We processed the alignment output with trimAL (Capella-Gutierrez et al. 2009) to remove poorly aligned regions. For phylogenetic analysis, we used IQ-TREE 2 (Minh et al. 2020), applying the LG + I + G amino acid substitution model (Le et al. 2008) and performing 1000 replicates of UFBoot (Hoang et al. 2018) and SH-aLRT (Guindon et al. 2010) to assess branch support. Unrooted and circular cladogram outputs were produced using Dendroscope (Huson and Scornavacca 2012).

Synteny Analysis of Anuran Genome Assemblies

We retrieved anuran genome assemblies from NCBI for synteny analysis, selecting only those labeled as annotated representative assemblies. Using Genome Data Viewer (Rangwala et al. 2021), we manually inspected these assemblies for conserved synteny blocks around *PLCZ1* and *PLCD4*. Additionally, we obtained unannotated chromosome assemblies to detect *PLCZ1* synteny blocks in species from the Pipidae family: the Zaire dwarf clawed frog (*H. boettgeri*) and the Marsabit clawed frog (*Xenopus borealis*). Here, synteny blocks were identified using tblastn with protein queries from *X. tropicalis* (for proteins other than PLCZ1) and *S. bombifrons* (for PLCZ1). The sequences were annotated with miniprot (Li 2023) and verified through blastx reciprocal best hits. For visualizing local synteny, we aligned sequences in the same gene order, using gene annotations provided by NCBI (for annotated assemblies) or miniprot (for assemblies without annotation).

Animals

Xenopus laevis adults were obtained commercially (Nasco) and kept in a controlled environment with a 12-h light/dark cycle at 20 °C. Sexually mature *X. laevis* males were euthanized by immersing them in a solution of tricaine-S (3.6 g/L, pH 7.4) for 30 min.

RNA Isolation

To obtain RNA, testes were removed from 3 euthanized *X. laevis* males and carefully cleaned them to remove fat and vascular tissue. We prepared tissue for RNA isolation by freezing it with liquid nitrogen and grinding it into a powder with a mortar and pestle. We then isolated RNA following instructions provided by RNeasy and QIAshredder kits (QIAgen).

RNA-seq Library Preparation and Data Acquisition

Before preparing the RNA-seq library, we first determined the integrity of the RNA using electrophoresis and measured its concentration by Qubit (Life Technologies). We then used Illumina TruSeq mRNA kit (Illumina) with modified protocol: SuperScript IV (Invitrogen) was used for first strand synthesis, the library was amplified with 10 cycles of PCR, and the amplified library was cleaned up with 35 µL AMPureXP beads (Beckman Coulter). The library was sequenced with 75 bp paired-end mRNA reads on an Illumina NextSeq500 platform with a Mid Output 150 flowcell (Illumina).

RNA-seq Analysis

Sequencing reads were uploaded to the public server at usegalaxy.org (Afgan et al. 2018). The reads were then aligned to the *X. laevis* genome (version 10.1) using HISAT2 (Galaxy version 2.2.1 + galaxy0) with default settings for paired reads. Next, aligned fragments were mapped and quantified with featureCounts (Galaxy version

2.0.1 + galaxy2) (Liao et al. 2014) using the Xenbase gene model as a reference.

BLAST Search for Unmapped *PLCZ1*

Command line BLASTx was used to search unmapped RNA-seq reads against a custom database containing PLCZ1 protein sequences. We filtered hits using an *E*-value cutoff of 10^{-6}, which produced 360 reads. We then aligned these reads to the translated nucleotide sequence of *PLCZ1* from a tree frog *P. bahiana*, which was excluded from the initial database. This produced a noncontiguous alignment covering residues 170 to 654 of the protein. We then cross-validated the identity of the aligned reads using a multiple query BLAST reciprocal best hits search against amphibian sequences from the nonredundant nucleotide (nt) database.

Comparative Transcriptome Analysis

To compare transcript levels, we took the average of 3 individual experiments and reported transcript abundance as the number of transcripts per million. We deposited this data with the NCBI Gene Expression Omnibus (Edgar et al. 2002), which can be accessed using accession number GSE224304. To ensure that our data could be compared with previously existing data, we matched the transcriptome of our dataset against a GEO dataset for *X. laevis* (J strain) (GSE73419) (Session et al. 2016). We identified 13,277 genes for direct comparison, which we then ranked and compared using Spearman's rank correlation in Prism (GraphPad).

To compare the expression of PLC subtypes in the testes of different organisms, we obtained GEO data for *X. laevis* (J strain) (GSE73419), *X. tropicalis* (nigerians) (GSM5230669), *B. orientalis* (GSE163874), and *Mus musculus* (GSE181426). Datasets were used as provided, except GSE181426, which was annotated and converted to transcripts per million using data from BioMart (19144180). We processed the expression data using a $\log_2$ transformation and created a heatmap using Prism (GraphPad) to visualize the interspecies comparison.

Supplementary Material

Supplementary material is available at *Genome Biology and Evolution* online.

Acknowledgments

We thank D. Summerville for excellent technical assistance and M.T. Lee for stimulating conversations.

Author Contributions

Rachel E. Bainbridge, Joel C. Rosenbaum, Anne E. Carlson (Conceptualization), Rachel E. Bainbridge, Joel C. Rosenbaum, Paushaly Sau, Anne E. Carlson (Data curation), Rachel E. Bainbridge, Joel C. Rosenbaum (Formal analysis), Rachel E. Bainbridge, Joel C. Rosenbaum, Anne E. Carlson (Investigation), Rachel E. Bainbridge, Joel C. Rosenbaum (Methodology), Rachel E. Bainbridge, Joel C. Rosenbaum, Anne E. Carlson (Project administration), Rachel E. Bainbridge, Joel C. Rosenbaum, Anne E. Carlson (Resources), Rachel E. Bainbridge, Joel C. Rosenbaum, Anne E. Carlson (Visualization), Rachel E. Bainbridge, Joel C. Rosenbaum, Anne E. Carlson (Writing—original draft), and Rachel E. Bainbridge, Joel C. Rosenbaum, Paushaly Sau, Anne E. Carlson (Writing—reviewing & editing).

Funding

This work was supported by National Institute for General Medical Sciences grants 1R35GM153270 and 1R01GM125638 (NIH, USA) to A.E.C. and a grant from the Office of Research, Health Sciences, University of Pittsburgh to J.C.R.

Conflict of Interest

The authors declare no competing interests.

Data Availability

The datasets generated and/or analyzed during the current study are available in the Gene Expression Omnibus, which can be accessed using accession number GSE224304.

Literature Cited

Aarabi M, Qin Z, Xu W, Mewburn J, Oko R. Sperm-borne protein, PAWP, initiates zygotic development in *Xenopus laevis* by eliciting intracellular calcium release. Mol Reprod Dev. 2010:77(3):249–256. https://doi.org/10.1002/mrd.21140.

Afgan E, Baker D, Batut B, van den Beek M, Bouvier D, Cech M, Chilton J, Clements D, Coraor N, Grüning BA, et al. The Galaxy platform for accessible, reproducible and collaborative biomedical analyses: 2018 update. Nucleic Acids Res. 2018:46(W1):W537–W544. https://doi.org/10.1093/nar/gky379.

Agarwal A, Sharma R, Durairajanayagam D, Cui Z, Ayaz A, Gupta S, Willard B, Gopalan B, Sabanegh E. Spermatozoa protein alterations in infertile men with bilateral varicocele. Asian J Androl. 2016:18(1):43–53. https://doi.org/10.4103/1008-682X.153848.

Bedford-Guaus SJ, McPartlin LA, Xie J, Westmiller SL, Buffone MG, Roberson MS. Molecular cloning and characterization of phospholipase C zeta in equine sperm and testis reveals species-specific differences in expression of catalytically active protein. Biol Reprod. 2011:85(1):78–88. https://doi.org/10.1095/biolreprod.110.089466.

Bowes JB, Snyder KA, Segerdell E, Jarabek CJ, Azam K, Zorn AM, Vize PD. Xenbase: gene expression and improved integration. Nucleic

Acids Res. 2010:38(suppl_1):D607–D612. https://doi.org/10.1093/nar/gkp953.
Capella-Gutierrez S, Silla-Martinez JM, Gabaldon T. trimAl: a tool for automated alignment trimming in large-scale phylogenetic analyses. Bioinformatics. 2009:25(15):1972–1973. https://doi.org/10.1093/bioinformatics/btp348.
Carlson KB, Wcisel DJ, Ackerman HD, Romanet J, Christiansen EF, Niemuth JN, Williams C, Breen M, Stoskopf MK, Dornburg A, et al. Transcriptome annotation reveals minimal immunogenetic diversity among Wyoming toads, *Anaxyrus baxteri*. Conserv Genet. 2022:23(4):669–681. https://doi.org/10.1007/s10592-022-01444-8.
Coward K, Ponting CP, Chang HY, Hibbitt O, Savolainen P, Jones KT, Parrington J. Phospholipase Cz, the trigger of egg activation in mammals, is present in a non-mammalian species. Reproduction. 2005:130(2):157–163. https://doi.org/10.1530/rep.1.00707.
Cox LJ, Larman MG, Saunders CM, Hashimoto K, Swann K, Lai FA. Sperm phospholipase Czeta from humans and cynomolgus monkeys triggers Ca^{2+} oscillations, activation and development of mouse oocytes. Reproduction. 2002:124(5):611–623. https://doi.org/10.1530/rep.0.1240611.
Crossley I, Swann K, Chambers E, Whitaker M. Activation of sea urchin eggs by inositol phosphates is independent of external calcium. Biochem J. 1988:252(1):257–262. https://doi.org/10.1042/bj2520257.
Denninger P, Bleckmann A, Lausser A, Vogler F, Ott T, Ehrhardt DW, Frommer WB, Sprunck S, Dresselhaus T, Grossmann G. Male-female communication triggers calcium signatures during fertilization in Arabidopsis. Nat Commun. 2014:5(1):4645. https://doi.org/10.1038/ncomms5645.
Dong JB, Tang TS, Sun FZ. Xenopus and chicken sperm contain a cytosolic soluble protein factor which can trigger calcium oscillations in mouse eggs. Biochem Biophys Res Commun. 2000:268(3):947–951. https://doi.org/10.1006/bbrc.2000.2218.
Edgar R, Domrachev M, Lash AE. Gene Expression Omnibus: NCBI gene expression and hybridization array data repository. Nucleic Acids Res. 2002:30(1):207–210. https://doi.org/10.1093/nar/30.1.207.
Ferlin A, Menegazzo M, Gianesello L, Selice R, Foresta C. Effect of relaxin on human sperm functions. J Androl. 2012:33(3):474–482. https://doi.org/10.2164/jandrol.110.012625.
Fukami K, Nakao K, Inoue T, Kataoka Y, Kurokawa M, Fissore RA, Nakamura K, Katsuki M, Mikoshiba K, Yoshida N, et al. Requirement of phospholipase Cdelta4 for the zona pellucida-induced acrosome reaction. Science. 2001:292(5518):920–923. https://doi.org/10.1126/science.1059042.
Gilkey JC, Jaffe LF, Ridgway EB, Reynolds GT. A free calcium wave traverses the activating egg of the medaka, *Oryzias latipes*. J Cell Biol. 1978:76(2):448–466. https://doi.org/10.1083/jcb.76.2.448.
Grey RD, Bastiani MJ, Webb DJ, Schertel ER. An electrical block is required to prevent polyspermy in eggs fertilized by natural mating of *Xenopus laevis*. Dev Biol. 1982:89(2):475–484. https://doi.org/10.1016/0012-1606(82)90335-9.
Guindon S, Dufayard JF, Lefort V, Anisimova M, Hordijk W, Gascuel O. New algorithms and methods to estimate maximum-likelihood phylogenies: assessing the performance of PhyML 3.0. Syst Biol. 2010:59(3):307–321. https://doi.org/10.1093/sysbio/syq010.
Harada Y, Kawazoe M, Eto Y, Ueno S, Iwao Y. The Ca^{2+} increase by the sperm factor in physiologically polyspermic newt fertilization: its signaling mechanism in egg cytoplasm and the species-specificity. Dev Biol. 2011:351(2):266–276. https://doi.org/10.1016/j.ydbio.2011.01.003.
Harada Y, Matsumoto T, Hirahara S, Nakashima A, Ueno S, Oda S, Miyazaki S, Iwao Y. Characterization of a sperm factor for egg activation at fertilization of the newt *Cynops pyrrhogaster*. Dev Biol. 2007:306(2):797–808. https://doi.org/10.1016/j.ydbio.2007.04.019.
Hime PM, Lemmon AR, Lemmon ECM, Prendini E, Brown JM, Thomson RC, Kratovil JD, Noonan BP, Pyron RA, Peloso PLV, et al. Phylogenomics reveals ancient gene tree discordance in the amphibian tree of life. Syst Biol. 2021:70(1):49–66. https://doi.org/10.1093/sysbio/syaa034.
Hoang DT, Chernomor O, von Haeseler A, Minh BQ, Vinh LS. UFBoot2: improving the ultrafast bootstrap approximation. Mol Biol Evol. 2018:35(2):518–522. https://doi.org/10.1093/molbev/msx281.
Houston DW, King ML. A critical role for Xdazl, a germ plasm-localized RNA, in the differentiation of primordial germ cells in Xenopus. Development. 2000:127(3):447–456. https://doi.org/10.1242/dev.127.3.447.
Huang Y, Li X, Sun X, Yao J, Gao F, Wang Z, Hu J, Wang Z, Ouyang B, Tu X, et al. Anatomical transcriptome atlas of the male mouse reproductive system during aging. Front Cell Dev Biol. 2021:9:782824. https://doi.org/10.3389/fcell.2021.782824.
Huson DH, Scornavacca C. Dendroscope 3: an interactive tool for rooted phylogenetic trees and networks. Syst Biol. 2012:61(6):1061–1067. https://doi.org/10.1093/sysbio/sys062.
Ito M, Shikano T, Oda S, Horiguchi T, Tanimoto S, Awaji T, Mitani H, Miyazaki S. Difference in Ca^{2+} oscillation-inducing activity and nuclear translocation ability of PLCZ1, an egg-activating sperm factor candidate, between mouse, rat, human, and medaka fish. Biol Reprod. 2008:78(6):1081–1090. https://doi.org/10.1095/biolreprod.108.067801.
Jaffe LA. First messengers at fertilization. J Reprod Fertil Suppl. 1990:42:107–116.
Jaffe LF. Sources of calcium in egg activation: a review and hypothesis. Dev Biol. 1983:99(2):265–276. https://doi.org/10.1016/0012-1606(83)90276-2.
Kadamur G, Ross EM. Mammalian phospholipase C. Annu Rev Physiol. 2013:75(1):127–154. https://doi.org/10.1146/annurev-physiol-030212-183750.
Kang W, Harada Y, Yamatoya K, Kawano N, Kanai S, Miyamoto Y, Nakamura A, Miyado M, Hayashi Y, Kuroki Y, et al. Extra-mitochondrial citrate synthase initiates calcium oscillation and suppresses age-dependent sperm dysfunction. Lab Invest. 2020:100(4):583–595. https://doi.org/10.1038/s41374-019-0353-3.
Katoh K, Standley DM. MAFFT multiple sequence alignment software version 7: improvements in performance and usability. Mol Biol Evol. 2013:30(4):772–780. https://doi.org/10.1093/molbev/mst010.
Kierszenbaum A, Tres LL. Structural and transcriptional features of the mouse spermatid genome. J Cell Biol. 1975:65(2):258–270. https://doi.org/10.1083/jcb.65.2.258.
Kline D. Calcium-dependent events at fertilization of the frog egg: injection of a calcium buffer blocks ion channel opening, exocytosis, and formation of pronuclei. Dev Biol. 1988:126(2):346–361. https://doi.org/10.1016/0012-1606(88)90145-5.
Komondor KM, Bainbridge RE, Sharp KG, Iyer AR, Rosenbaum JC, Carlson AE. TMEM16A activation for the fast block to polyspermy in the African clawed frog does not require conventional activation of egg PLCs. J Gen Physiol. 2023:155(10):e202213258. https://doi.org/10.1085/jgp.202213258.
Le SQ, Lartillot N, Gascuel O. Phylogenetic mixture models for proteins. Philos Trans R Soc Lond B Biol Sci. 2008:363(1512):3965–3976. https://doi.org/10.1098/rstb.2008.0180.
Li H. Protein-to-genome alignment with miniprot. Bioinformatics. 2023:39:btad014. https://doi.org/10.1093/bioinformatics/btad014.

Liao Y, Smyth GK, Shi W. featureCounts: an efficient general purpose program for assigning sequence reads to genomic features. Bioinformatics. 2014:30(7):923–930. https://doi.org/10.1093/bioinformatics/btt656.

Ma WJ, Veltsos P, Sermier R, Parker DJ, Perrin N. Evolutionary and developmental dynamics of sex-biased gene expression in common frogs with proto-Y chromosomes. Genome Biol. 2018:19(1):156. https://doi.org/10.1186/s13059-018-1548-4.

Maccarinelli F, Regoni M, Carmona F, Poli M, Meyron-Holtz EG, Arosio P. Mitochondrial ferritin deficiency reduces male fertility in mice. Reprod Fertil Dev. 2017:29(10):2005–2010. https://doi.org/10.1071/RD16348.

Matsunami M, Suzuki M, Haramoto Y, Fukui A, Inoue T, Yamaguchi K, Uchiyama I, Mori K, Tashiro K, Ito Y, et al. A comprehensive reference transcriptome resource for the Iberian ribbed newt *Pleurodeles waltl*, an emerging model for developmental and regeneration biology. DNA Res. 2019:26(3):217–229. https://doi.org/10.1093/dnares/dsz003.

Minh BQ, Schmidt HA, Chernomor O, Schrempf D, Woodhams MD, von Haeseler A, Lanfear R. IQ-TREE 2: new models and efficient methods for phylogenetic inference in the genomic era. Mol Biol Evol. 2020:37(5):1530–1534. https://doi.org/10.1093/molbev/msaa015.

Mizushima S, Hiyama G, Shiba K, Inaba K, Dohra H, Ono T, Shimada K, Sasanami T. The birth of quail chicks after intracytoplasmic sperm injection. Development. 2014:141(19):3799–3806. https://doi.org/10.1242/dev.111765.

Mizushima S, Takagi S, Ono T, Atsumi Y, Tsukada A, Saito N, Shimada K. Possible role of calcium on oocyte development after intracytoplasmic sperm injection in quail (*Coturnix japonica*). J Exp Zool A Ecol Genet Physiol. 2007:307(11):647–653. https://doi.org/10.1002/jez.a.418.

Nomikos M, Blayney LM, Larman MG, Campbell K, Rossbach A, Saunders CM, Swann K, Lai FA. Role of phospholipase C-zeta domains in Ca^{2+}-dependent phosphatidylinositol 4,5-bisphosphate hydrolysis and cytoplasmic Ca^{2+} oscillations. J Biol Chem. 2005:280(35):31011–31018. https://doi.org/10.1074/jbc.M500629200.

Nomikos M, Kashir J, Lai FA. The role and mechanism of action of sperm PLC-zeta in mammalian fertilisation. Biochem J. 2017:474(21):3659–3673. https://doi.org/10.1042/BCJ20160521.

Nomikos M, Sanders JR, Kashir J, Sanusi R, Buntwal L, Love D, Ashley P, Sanders D, Knaggs P, Bunkheila A, et al. Functional disparity between human PAWP and PLCzeta in the generation of Ca^{2+} oscillations for oocyte activation. Mol Hum Reprod. 2015:21(9):702–710. https://doi.org/10.1093/molehr/gav034.

Nomikos M, Sanders JR, Theodoridou M, Kashir J, Matthews E, Nounesis G, Lai FA, Swann K. Sperm-specific post-acrosomal WW-domain binding protein (PAWP) does not cause Ca^{2+} release in mouse oocytes. Mol Hum Reprod. 2014:20(10):938–947. https://doi.org/10.1093/molehr/gau056.

Nomikos M, Theodoridou M, Elgmati K, Parthimos D, Calver BL, Buntwal L, Nounesis G, Swann K, Lai FA. Human PLCzeta exhibits superior fertilization potency over mouse PLCzeta in triggering the Ca(2+) oscillations required for mammalian oocyte activation. Mol Hum Reprod. 2014:20(6):489–498. https://doi.org/10.1093/molehr/gau011.

Oikawa M, Simeone A, Hormanseder E, Teperek M, Gaggioli V, O'Doherty A, Falk E, Sporniak M, D'Santos C, Franklin VN, et al. Epigenetic homogeneity in histone methylation underlies sperm programming for embryonic transcription. Nat Commun. 2020:11(1):3491. https://doi.org/10.1038/s41467-020-17238-w.

Rangwala SH, Kuznetsov A, Ananiev V, Asztalos A, Borodin E, Evgeniev V, Joukov V, Lotov V, Pannu R, Rudnev D, et al. Accessing NCBI data using the NCBI Sequence Viewer and Genome Data Viewer (GDV). Genome Res. 2021:31(1):159–169. https://doi.org/10.1101/gr.266932.120.

Rhee SG. Regulation of phosphoinositide-specific phospholipase C. Annu Rev Biochem. 2001:70(1):281–312. https://doi.org/10.1146/annurev.biochem.70.1.281.

Ross PJ, Beyhan Z, Iager AE, Yoon SY, Malcuit C, Schellander K, Fissore RA, Cibelli JB. Parthenogenetic activation of bovine oocytes using bovine and murine phospholipase C zeta. BMC Dev Biol. 2008:8(1):16. https://doi.org/10.1186/1471-213X-8-16.

Runft LL, Jaffe LA, Mehlmann LM. Egg activation at fertilization: where it all begins. Dev Biol. 2002:245(2):237–254. https://doi.org/10.1006/dbio.2002.0600.

Runft LL, Watras J, Jaffe LA. Calcium release at fertilization of *Xenopus* eggs requires type I IP_3 receptors, but not SH2 domain-mediated activation of PLCγ or G_q-mediated activation of PLCβ. Dev Biol. 1999:214(2):399–411. https://doi.org/10.1006/dbio.1999.9415.

Sakaue T, Takeuchi K, Maeda T, Yamamoto Y, Nishi K, Ohkubo I. Factor H in porcine seminal plasma protects sperm against complement attack in genital tracts. J Biol Chem. 2010:285(3):2184–2192. https://doi.org/10.1074/jbc.M109.063495.

Sato K, Tokmakov AA, Iwasaki T, Fukami Y. Tyrosine kinase-dependent activation of phospholipase Cgamma is required for calcium transient in Xenopus egg fertilization. Dev Biol. 2000:224(2):453–469. https://doi.org/10.1006/dbio.2000.9782.

Saunders CM, Larman MG, Parrington J, Cox LJ, Royse J, Blayney LM, Swann K, Lai FA. PLC zeta: a sperm-specific trigger of Ca(2+) oscillations in eggs and embryo development. Development. 2002:129(15):3533–3544. https://doi.org/10.1242/dev.129.15.3533.

Session AM, Uno Y, Kwon T, Chapman JA, Toyoda A, Takahashi S, Fukui A, Hikosaka A, Suzuki A, Kondo M, et al. Genome evolution in the allotetraploid frog *Xenopus laevis*. Nature. 2016:538(7625):336–343. https://doi.org/10.1038/nature19840.

Shechter D, Nicklay JJ, Chitta RK, Shabanowitz J, Hunt DF, Allis CD. Analysis of histones in *Xenopus laevis*. I. A distinct index of enriched variants and modifications exists in each cell type and is remodeled during developmental transitions. J Biol Chem. 2009:284(2):1064–1074. https://doi.org/10.1074/jbc.M807273200.

Smrcka AV, Hepler JR, Brown KO, Sternweis PC. Regulation of polyphosphoinositide-specific phospholipase C activity by purified Gq. Science. 1991:251(4995):804–807. https://doi.org/10.1126/science.1846707.

Steinhardt R, Zucker R, Schatten G. Intracellular calcium release at fertilization in the sea urchin egg. Dev Biol. 1977:58(1):185–196. https://doi.org/10.1016/0012-1606(77)90084-7.

Swann K. Sperm factors and egg activation: PLCzeta as the sperm factor that activates eggs: 20 years on. Reproduction. 2022:164(1):E1–E4. https://doi.org/10.1530/REP-22-0148.

Swann K, Lai FA. Egg activation at fertilization by a soluble sperm protein. Physiol Rev. 2016:96(1):127–149. https://doi.org/10.1152/physrev.00012.2015.

Swann K, Ozil JP. Dynamics of the calcium signal that triggers mammalian egg activation. Int Rev Cytol. 1994:152:183–222. https://doi.org/10.1016/S0074-7696(08)62557-7.

Wang Z, Gerstein M, Snyder M. RNA-Seq: a revolutionary tool for transcriptomics. Nat Rev Genet. 2009:10(1):57–63. https://doi.org/10.1038/nrg2484.

Whitaker M. Calcium at fertilization and in early development. Physiol Rev. 2006:86(1):25–88. https://doi.org/10.1152/physrev.00023.2005.

Wozniak KL, Carlson AE. Ion channels and signaling pathways used in the fast polyspermy block. Mol Reprod Dev. 2020:87(3):350–357. https://doi.org/10.1002/mrd.23168.

Wozniak KL, Phelps WA, Tembo M, Lee MT, Carlson AE. The TMEM16A channel mediates the fast polyspermy block in

Xenopus laevis. J Gen Physiol. 2018:150(9):1249–1259. https://doi.org/10.1085/jgp.201812071.
Wozniak KL, Tembo M, Phelps WA, Lee MT, Carlson AE. PLC and IP3-evoked Ca(2+) release initiate the fast block to polyspermy in *Xenopus laevis* eggs. J Gen Physiol. 2018:150(9):1239–1248. https://doi.org/10.1085/jgp.201812069.
Wu AT, Sutovsky P, Manandhar G, Xu W, Katayama M, Day BN, Park KW, Yi YJ, Xi YW, Prather RS, et al. PAWP, a sperm-specific WW domain-binding protein, promotes meiotic resumption and pronuclear development during fertilization. J Biol Chem. 2007:282(16):12164–12175. https://doi.org/10.1074/jbc.M609132200.
Xiong J, Lv Y, Huang Y, Liu Q. The first transcriptome assembly of Yenyuan stream salamander (*Batrachuperus yenyuanensis*) provides novel insights into its molecular evolution. Int J Mol Sci. 2019:20(7):1529. https://doi.org/10.3390/ijms20071529.
Yoneda A, Kashima M, Yoshida S, Terada K, Nakagawa S, Sakamoto A, Hayakawa K, Suzuki K, Ueda J, Watanabe T. Molecular cloning, testicular postnatal expression, and oocyte-activating potential of porcine phospholipase Czeta. Reproduction. 2006:132(3):393–401. https://doi.org/10.1530/rep.1.01018.

Associate editor: Selene Fernandez-Valverde